N-vinylpyrrolidone copolymer encapsulates AlN powders for anti-hydrolysis

Jianjun Xie (xiejianjun@shu.edu.cn)
Shun Wang
Yu Wang
Tun Wang
Junhong Li
Guangcheng Yu
Lei Zhang
Fang Lei
Ying Shi

Research Article

Keywords: Aluminum nitride powders, Surface modification, N-vinylpyrrolidone copolymers, Titanate coupling agents

Posted Date: April 13th, 2022

DOI: https://doi.org/10.21203/rs.3.rs-1537515/v1

Abstract

Hydrolysis resistance of aluminum nitride (AlN) particles can be achieved by chemically grafting AlN powders to titanate coupling agents (KR-238S) and poly (N-vinyl pyrrolidone-co-itaconic acid) (NVP-IA). The modified AlN (M-AlN) powders were characterized by transmission electron microscopy, X-ray photoelectron spectroscopy, Fourier transform infrared spectroscopy, X-ray diffraction, scanning electron microscopy, zeta potential and thermal gravimetric analysis. The TEM results showed that a wrapping layer approximately 20 nm thick was formed on the surface of the AlN powders, forming a core-shell structure to isolate contact with water molecules. During the anti-hydrolysis test, $Al(OH)_3$ was formed within 12 h of the original AlN powders being hydrolyzed, whereas the modified AlN particles maintained their morphology and crystal structure for 276 h. The zeta analysis demonstrates that M-AlN has stronger absolute zeta values. The results obtained from the thermal gravimetric analysis also revealed that NVP-IA vaporizes completely at high temperatures with no effect on the sintered AlN ceramics.

1 Introduction

Commonly used packaging substrate materials can be categorized into three main categories: plastics, metal composites and ceramics. AlN ceramics possess the characteristics of high thermal conductivity, low dielectric constant, electrical insulation and non-toxicity[1–6]. Recently, it has become a popular substrate packaging material for modern power devices and large-scale integrated circuit chip-related component devices. [7–10]. Casting, slurry molding, and injection molding are the most common industrial processes use to prepar AlN blocks and sheets [11]. These processes typically involve the use of water-based pastes or water-soluble binders. AlN powders are highly susceptible to hydrolysis with water molecules, forming $Al(OH)_3$ or AlOOH, which can drastically increase the pH of the slurry [12–14].

Therefore, there is an urgent need to improve the surface hydrolysis resistance of AlN powders. A good surface modifier should satisfy the requirements of covering AlN particles, and maintaining a stable suspension state[15, 16]. The research on the hydrolysis mechanism and kinetics of AlN powders has demonstrated that the introduction of long molecular chain organics or inorganic acids as surface modification ingredients can effectively improve and limit the hydrolysis of AlN [17–19]. Krnel [20] applied phosphoric acid to modify AlN powders and proposed that a phosphoric acid molecular layer was formed on the surface of AlN powders by the esterification reaction of hydroxyl groups, which may clearly surround AlN to resist hydrolysis within 72 hours. However, the phosphorus (P) is arduous to remove during the subsequent sintering process of AlN ceramics, causing the ceramics to have a negative impact. Therefore, additional methods for preventing AlN powder hydrolysis are urgently required.

Amphiphilic random copolymers are formed by the random copolymerization of hydrophilic and hydrophobic monomers, in which hydrophilic and hydrophobic chain segments are randomly arranged according to a certain probability, they are also called polymeric surfactants because they lower the surface tension of water. N-vinylpyrrolidone (NVP) is amphiphilic and belongs to the class of lactams[21, 22]. Itaconic acid (IA) contains an unsaturated double bond and two active carboxyl groups. The random

copolymerization of these two monomers to form N-vinylpyrrolidone-co-itaconic acid copolymer (NVP-IA) has better water solubility and high stability, which makes the copolymer have good practical value in surface modification, water treatment, and medicine. The titanate coupling agent is a new type of auxiliary agent in the past 30 years, which can combine organic polymer materials and inorganic materials through physical or chemical action to form a transition layer with a certain thickness. In 1977, Monte S J [23] proposed the chemical bonding theory, which titanate coupling agent can form a chemical bond between inorganic materials and organic polymers through chemical bonds, and form an organic active monolayer between the two-phase interface. Using a titanate coupling agent as an intermediate layer to chemically bond NVP-IA on the surface of AlN particles to form an encapsulation layer, can not only solve the hydrolysis resistance of AlN powder, but also improve the dispersion of modified AlN powders in water.

In this study, NVP-IA copolymer which contain carboxylic acids functional groups were reacted with the hydroxyl groups of AlN powders to form a coating layer. The structure of raw AlN (R-AlN) and modified AlN (M-AlN) powders were observed under Transmission electron microscope (TEM) and EDS to investigate the change of element content in the coating layer, and the chemical bonds of AlN powders were measured by Fourier transform infrared spectroscopy (FT-IR) and X-ray photoelectron spectrometer (XPS). In order to evaluate the hydrolysis resistance, the pH change of the aqueous solution of AlN suspension was measured, and the micromorphological changes of the powders were observed by scanning electron microscopy (SEM), and the crystal phase were showed by X-ray diffraction (XRD). Finally, the dispersibility of M-AlN powders were tested by Zeta potential, and Thermogravimetric Analysis (TG) was used to find whether NVP-IA in M-AlN is easily removed at high temperature without affecting the AlN ceramic properties.

2 Experimental Methods

2.1 Raw Materials

AlN powders (Tokuyama, Japan, average particle size = 0.8 μm) were used in this study. Titanate coupling agent (KR-238S) was used as coupling agent. N-vinylpyrrolidone-Itaconic acid copolymer (NVP-IA) (Yoking Corp., China) was used as coating agents. Absolute ethanol (mass fraction ≥ 99.5%, chemically pure) was used as solvent.

2.2 Sample Preparation

10g raw AlN powders (R-AlN) was dispersed in 50 ml anhydrous ethanol. Add H_2SO_4 to adjust the pH to 4, and then add 1 ml H_2O_2 to obtain hydroxylated AlN powders. In the modification method of titanate coupling agent, 0.3 g titanate coupling agent was ultrasonically dispersed in 20 ml absolute ethanol, added to the suspension of hydroxylated AlN powders, and stirred at 80°C for 4 hours to obtain an intermediate AlN powders. Then 1g of NVP-IA polymer was dispersed in 30 ml absolute ethanol and

added to the intermediate suspension, and continued to react at 80°C for 4 hours, centrifuged, washed, and dried to obtain the modified reaction product (M-AlN).

2.3 Performance testing

The microstructure of the powders surface and perform element scanning were respectively observed under the Transmission electron microscope (TEM, JEOL, JEM F200). The surface functional groups of R-AlN and M-AlN were tested by Fourier transform infrared spectroscopy (FT-IR, Thermo Scientific Nicolet iS 50, ATR) and X-ray photoelectron spectrometer (XPS, Japan, Kratos, AXIS Ultra DLD). R-AlN and M-AlN powders were respectively dispersed in deionized water, it is measured the relationship between pH value change and time at 25°C. And the morphology changes of the powders were observed by scanning electron microscopy (SEM, EM-30, COXEM) to explore whether M-AlN was hydrolyzed. The crystal phase was observed by X-ray diffraction (XRD, Rigaku, D/MAX2200, 3KW). The dispersion and stability of the powders were analyzed by measuring the surface zeta potential (zata, Malvern, zetasizer Nano ZES). To observe the thermal weight loss of M-AlN under nitrogen atmosphere (TG, METTLER, TGA/DSC3+).

3 Results And Discussion

3.1 Morphology and Structural characterization

In order to clearly observe the microscopic morphology of the R-AlN and M-AlN powders surfaces, the thickness of the coating layer was observed by TEM (as shown in Fig. 2). The R-AlN powders have an oxide layer on the surface due to long-term storage, with a thickness of 5.59 nm (as shown in Fig. 2b). In addition to the presence of Al, N elements, the R-AlN particles also uniformly distribute oxygen elements (as shown in Fig. 3). The oxygen element comes from the oxide layer on the surface, forming hydroxyl groups homogeneously distributed on the surface of the AlN powders, and these hydroxyl groups are the active sites for the reaction with NVP-IA. Figure 2c and 2d shows the surface of the modified AlN powders is coated with a layer of NVP-IA with a thickness of about 20 nm. And it is clearly observed that there is a silk-like substance implicated between the AlN powders. This is because NVP-IA is a macromolecular polymer, and the molecular chains are easily entangled with each other to stick multiple powders together. Figure 2d further shows the thickness of the local coating layer of the M-AlN powder, which ranged from 17.21 nm to 19.91 nm. From the M-AlN powders element distribution diagram in Fig. 4, it can be observed that in addition to Al and N, there are also C, O elements from the NVP-IA polymer, and P elements from the titanate coupling agent. It can be observed from Fig. 4d that the filaments connected between the spherical particles do not contain Al and N, but it can be clearly noticed that the main element is carbon. The C is derived from the carbon chain in NVP-IA, further confirming that this silky substance is NVP-IA. Figure 5 is a line scan of a partial magnification of R-AlN and M-AlN powders. In the R-AlN powder, the Al and N increased significantly at the edge of the powder, and the oxygen element began to increase slightly which originated from oxide layer (as shown in Fig. 5a). When M-AlN was line-scanned into the cladding layer, the carbon content in the cladding layer increased markedly, with a slightly increased amount of oxygen and nitrogen elements (as shown in Fig. 5b). This indicates that the

main element of the cladding layer is carbon, as well as small amounts of nitrogen and oxygen, which corroborates with the elemental composition of the polymer NVP-IA. When continuing to scan into the interior of AlN particles, the weight percentage of carbon element decreases, and the content of Al and N increases obviously.

In order to explore the interaction between NVP-IA and the surface of AlN powders, the chemical structure of the powders was tested (as shown in Fig. 6). The NVP-IA, R-AlN and M-AlN were tested by using FT-IR spectroscopy in the range of 4000 – 400 cm^{-1}, respectively (as shown in Fig. 6a). In the infrared characteristic curve of NVP-IA, it can be observed that the -CH_2- stretching vibration peak at 2975 cm^{-1}, the band at 1718 cm^{-1} is assigned to the C = O stretching vibration of the carboxylic acid, 1659 cm^{-1} is attributed to the C = O of NVP, 1290 cm^{-1} is assigned to the C-N stretching vibration peak, and 1049 cm^{-1} attributed to the bending mode of hydroxyl groups of the carboxylic acid in IA. [24]. Characteristic peaks of R-AlN were identified, a strong Al-N vibration was observed at 500-900cm^{-1}, a sharp Al-N peak at 1332cm^{-1}, and the absorption bands of –OH stretching at 3339cm^{-1} appeared [25]. When R-AlN is wrapped with NVP-IA polymer, it is worth noting that the strong peaks at 1049 cm^{-1} were completely unobservable and instead the weak peaks at 1018cm^{-1} appeared of M-AlN, indicating a strong interaction between AlN particles and COOH of NVP-IA. These FT-IR spectral results confirm the successful grafting of polymers from the surface of AlN particles.

For more insight into the interactions between AlN and the NVP-IA, XPS measurements were performed on R-AlN and M-AlN to analyze the surface chemical structure and composition. Figure 6b shows the qualitative full spectrum analysis of R-AlN and M-AlN surfaces by XPS. In addition to Al 2P and N 1S, R-AlN also has C 1S and O 1S, among which the O 1S peak is the most noteworthy characteristic, indicating that the surface oxygen concentration of the R-AlN is relatively high, a large part of which is the result of atmospheric oxidation. A substantial amount of carbon is also being observed here, which is characteristic of uncleaned surfaces. M-AlN particles were performed on the areas around the peaks C 1S, O 1S, P 2P, Al 2P and N 1S. Upon the modification, the peak of C 1S increases remarkably from 33.12–61.30%. In contrast, the peak of Al 2P decreases substantially from 32.11–6.29%, and the peak of N 1S drop from 11.09–4.48% (Table 1). This is because XPS generally brings out photoelectron information within 10 nm of the surface, and the thickness of the M-AlN coating layer is mostly more than 10 nm, so the detected signals of Al and N are weakened, which come from the interior of the particles. Figure 6c shows the C 1s peak of R-AlN and M-AlN, fitted by a multipeak Lorentzian fitting program. The C 1S electron binding energy spectrum of R-AlN is derived from the contaminated carbon adsorbed in the air. High-resolution XPS scans of the C 1S peaks for the M-AlN can be deconvolved into four Gaussian-Lorentzian subpeaks, centered at 284.8 eV, 285.91 eV, 287.03 eV and 288.64 eV. Where 285.91 eV corresponds to the C-N chemical bond of the VP. The N 1S data and the fitted subpeaks from a sample of AlN are shown in Fig. 6c. The N 1S peaks of R-AlN can be determined as 396.48 eV and 398.25 eV, corresponding to Al-N and N-C, respectively. The intensity of the Al-N peak of M-AlN is significantly weaker compared to the R-AlN, and the 399.96 eV corresponds to the tertiary amine C-N bond of NVP-IA [22, 26, 27].

Table 1
XPS chemical composition of samples

Sample	Al 2P(at%)	N 1S(at%)	C 1S(at%)	O 1S(at%)	P 2P(at%)
R-AlN	32.11	11.09	33.12	23.68	\
M-AlN	6.29	4.48	61.30	26.54	1.39

3.2 Characteristics of hydrolysis resistance

A certain amount of AlN powders was soaked in deionized water, dispersed uniformly to form a suspension, and the hydrolysis resistance was measured at 25°C. In Fig. 7a, it can be found that the pH value of R-AlN powder increased rapidly within 12h, from 7.25 to 9.43, and reached 10.28 after 36h. The R-AlN suspension generated $Al(OH)_3$ and NH_3 at 25°C, and ammonia gas was partly dissolved in water to produce OH^-, leading to an increase in the pH of the suspension and partly released to produce an irritating odor, which was similar to the results of Knel's[20] study. The initial pH of the M-AlN suspension was 4.12, which was lower than R-AlN, due to the effect of two unsaturated carboxylic acids in itaconic acid. After soaking for 276 h, the pH of the M-AlN suspension maintained around 4.22, which was similar to the initial value. No irritating odor was produced during the whole process, indicating that M-AlN has good stability after long-term soaking in water. R-AlN, M-AlN, R-AlN soaked in water for 12 hours (R-AlN-12), and M-AlN soaked in water for 276 hours (M-AlN-276) were respectively subjected to XRD tests (as shown in Fig. 7b). Compared with the $Al(OH)_3$ standard card, the diffraction peaks of $Al(OH)_3$ can be observed in R-AlN-12, while the AlN diffraction peaks remain unchanged in M-AlN-276. This is the consistency with the pH change, where R-AlN is easily hydrolyzed to form Al(OH)3, while M-AlN has excellent resistance to hydrolysis.

Figure 8 is the SEM image and EDS mapping spectrum of the R-AlN powder. It can be found that the original powder is oval with a smooth surface, and some AlN particles agglomerate together to form large particles. After immersion in water for 12 h at 25°C, the R-AlN particles aggregated to form larger cluster sizes, which were hydrolyzed to form rod-like structures of about 2–5 μm in length (Fig. 8b). Compared to the Al element, the N distribution is substantially reduced, while the O element content is elevated. Table 2 shows that the Al, N, and O contents are 31.35%, 10.44%, and 58.11%, respectively. As shown in Fig. 9 of M-AlN particles, the NVP-IA macromolecular chains are easily cross-linked to form a network structure. After immersion in water for 276 h, M-AlN kept spherical morphology unchanged and did not produce a rod-like structure of $Al(OH)_3$. The Al, N elements were uniformly distributed, the C, O and P elements from the modifier were also present, with the contents of 10.84%, 2.15% and 0.31%, respectively (Table 2). This indicates that M-AlN particles has not undergone hydrolysis reaction with its excellent core-shell structure.

Table 2
EDS elements composition of samples

Sample	Al (at%)	N (at%)	C (at%)	O (at%)	P (at%)
R-AlN-12	31.35	10.44	\	58.11	\
M-AlN-276	46.56	40.14	10.84	2.15	0.31

3.3 Dispersion performance and thermal stability of modified powders

The zeta potential can reflect the dispersion behavior of powder particles in the water, The higher the Zeta potential of the particle surface, the greater the surface charge density, the stronger the electrostatic repulsion between the particles, and the more conducive to the stable dispersion of the slurry. When the pH of R-AlN is 7.3, the Zeta potential is 0 (Fig. 10a), and it is easy to attract each other through van der waals attraction to form clusters. Due to the large number of hydroxyl groups on the surface of R-AlN powders, it is positively electrically charged by adsorbing H^+ under acidic conditions, and negatively charged by adsorbing OH^- under alkaline conditions. There is a substantial amount of COOH exists on M-AlN surface, which is negatively charged after dissociation in water, thus resulting in an increase in the negative value of M-AlN. This caused a variation in the zeta potential, with a shift of the equipotential point toward the acidic range, which is located at pH = 4.2. At the equivalent base pH, the M-AlN powders had a relatively larger absolute value of zata potential, the double electric layer repulsion between the powders was strengthened, which was beneficial to improve the dispersion stability of the slurry. Figure 10b presents the thermal weight loss curves of M-AlN powders under nitrogen atmosphere. The weight loss of the specimens was observed to be 1.61% below 183°C, it was mainly due to the detachment of adsorbed water. The weight loss rate of M-AlN powders was accelerated in the region of 183–573°C with a weight loss ratio of 7.03%. The sample mass remained stable at 90.01% at 1100°C, which is in accordance with our initial additive of 10%. The NVP-IA is completely vaporized and removed before 1100°C, which has no influence on the sintered AlN ceramics.

4 Conclusion

In this study, we present the surface modification of pristine AlN powders with titanate coupling agents and NVP-IA polymers. The core-shell structures of water-soluble M-AlN were successfully observed, and their anti-hydrolytic effects were investigated. It is proved by TEM showed that the thickness of the protective layer is approximately 20 nanometers, which is uniformly distributed on the surface of the AlN particles and can function as a shield well and does not affect the crystal structure inside the particles. The R-AlN powders form a stick structure after being immersed in water at 25°C for 12 h, while the M-AlN maintained stability in water for 276 h. The absolute value of the zeta potential of the M-AlN suspension increased to 60 mV, which is favorable for the subsequent preparation of a uniformly dispersed slurry.

And TG analysis further demonstrated that NVP-IA vaporizes and is removed at high temperatures. The NVP-IA is an excellent surface modifier for AlN powders, and can effectively achieve anti-hydrolysis properties without influencing the subsequent ceramic sintering performance.

Declarations

Acknowledgement:

This work was supported by the Shanghai Municipal Natural Science Foundation, China (Granted no. 19ZR1418500) and National Natural Science Foundation of China (Granted no. 51172139).

Funding

This work was supported by the Shanghai Municipal Natural Science Foundation, China (Granted no. 19ZR1418500) and National Natural Science Foundation of China (Granted no. 51172139).

Competing Interests

The authors have no relevant financial or non-financial interests to disclose.

Author Contributions

All authors contributed to the study conception and design. Material preparation, data collection and analysis were performed by [Shun Wang], and [Guangcheng Yu]. The first draft of the manuscript was written by [Shun Wang] and all authors commented on previous versions of the manuscript. All authors read and approved the final manuscript.

References

1. A. Collange, P. Grosseau, B. Guilhot, Thermal Conductivity of Compacted AlN Samples. J. Eur. Ceram. Soc. **17**, 1897–1900 (1997)
2. X. Fang, L. Jiang, L. Pan, High-thermally conductive AlN-based microwave attenuating composite ceramics with spherical graphite as attenuating agent. J. Adv. Ceram. **10**, 301–319 (2021)
3. G.A. Slack, R.A. Tanzilli, R.O. Pohl, The intrinsic thermal conductivity of AlN. J. Phys. Chem. Solids **48**, 641–647 (1987)
4. T. Kusunose, T. Sekino, Improvement in fracture strength in electrically conductive AlN ceramics with high thermal conductivity. Ceram. Int. **42**, 13183–13189 (2016)
5. M. Ohashi, S. Kawakami, Y. Yokogawa, Spherical Aluminum Nitride Fillers for Heat-Conducting Plastic Packages. J. Am. Ceram. Soc. **88**, 2615–2618 (2005)
6. R. Yin, Y. Zhang, W. Zhao, Graphene platelets/aluminium nitride metacomposites with double percolation property of thermal and electrical conductivity. J. Eur. Ceram. Soc. **38**, 4701–4706 (2018)

7. X. Fang, L. Pan, S. Yin, Spherical glassy carbon/AlN microwave attenuating composite ceramics with high thermal conductivity and strong attenuation. Ceram. Int. **46**, 21505–21516 (2020)
8. J. Cheng, D. Agrawal, Y. Zhang, Development of Translucent Aluminum Nitride (AlN) Using Microwave Sintering Process. J. Electrochem. **9**, 67–71 (2002)
9. P.J. Rutkowski, D. Kata, Thermal properties of AlN polycrystals obtained by pulse plasma sintering method. J. Adv. Ceram. **2**, 180–184 (2013)
10. C. Yun, Y. Feng, T. Qiu, Mechanical, electrical, and thermal properties of graphene nanosheet/aluminum nitride composites. Ceram. Int. **41**, 8643–8649 (2015)
11. Q.Shang, Z.Wang, J., Li, Gel-tape-casting of aluminum nitride ceramics. J. Adv. Ceram. **6[1]**, 67–72 (2017)
12. A. Kocjan, A. Dakskobler, K. Krnel, The course of the hydrolysis and the reaction kinetics of AlN powder in diluted aqueous suspensions. J. Eur. Ceram. Soc. **31**, 815–823 (2011)
13. A. Kocjan, K. Krnel, T. Kosmač, The influence of temperature and time on the AlN powder hydrolysis reaction products. J. Eur. Ceram. Soc. **28**, 1003–1008 (2008)
14. S. Fukumoto, T. Hookabe, H. Tsubakino, Hydrolysis behavior of aluminum nitride in various solutions. J. Mater. Sci. **35**, 2743–2748 (2000)
15. I. Ganesh, S.M. Olhero, A.B. Araújo, Chemisorption of Phosphoric Acid and Surface Characterization of As Passivated AlN Powder Against Hydrolysis. Langmuir **24**, 5359–5365 (2008)
16. Y. Shimizu, J. Hatano, T. Hyodo, Ion-exchange loading of Yttrium acetate as a sintering aid on aluminum nitride powder via aqueous processing. J. Am. Ceram. Soc. **83**, 2793–2797 (2000)
17. H.T. Chiu, T. Sukachonmakul, M.T. Kuo, Surface modification of aluminum nitride by polysilazane and its polymer-derived amorphous silicon oxycarbide ceramic for the enhancement of thermal conductivity in silicone rubber composite. Appl. Surf. Sci. **292**, 928–936 (2014)
18. I. Ganesh, S.M. Olhero, J.M.F. Ferreira, Phosphoric acid treated AlN powder for aqueous processing of net-shape dense AlN andβ-SiAlON parts. Adv. Appl. Ceram. **108**, 111–117 (2013)
19. L.-H. Hu, Y.-K. Wang, S.-C. Wang, Aluminum nitride surface functionalized by polymer derived silicon oxycarbonitride ceramic for anti-hydrolysis. J. Alloys Compd. **772**, 828–833 (2019)
20. K. Krnel, T. Kristoffer, Protection of AlN powder against hydrolysis using aluminum dihydrogen phosphate. J. Eur. Ceram. Soc. 2075–2079 (2001)
21. L. Hao, K. Zhu, G. Lv, A comparative study of nanoscale poly N-(vinyl) pyrrole in polyvinyl butyral coatings for the anti-corrosion property of zinc: Nanotubes vs nanoparticles. Prog. Org. Coat. 136 (2019)
22. M. Contardi, D. Kossyvaki, P. Picone, Electrospun polyvinylpyrrolidone (PVP) hydrogels containing hydroxycinnamic acid derivatives as potential wound dressings. Chem. Eng. J. 409 (2021)
23. S.J. Monte, Functional Fillers for Plastics, ed. By M. Xanthos (Wiley, 2005), pp. 85–104
24. A. Baykal, N. Bıtrak, B. Ünal, Polyol synthesis of (polyvinylpyrrolidone) PVP–Mn_3O_4 nanocomposite. J. Alloys Compd. **502**, 199–205 (2010)

25. G. Yu, J. Xie, S. Wang, Non hydrolizable aluminum nitride powders surface modified by silicic acids. Ceram. Int. **47**, 29253–29260 (2021)
26. P. Motamedi, K. Cadien, XPS analysis of AlN thin films deposited by plasma enhanced atomic layer deposition. Appl. Surf. Sci. **315**, 104–109 (2014)
27. J. Wang, K. Zhang, S. Hao, Simultaneous reduction and surface functionalization of graphene oxide and the application for rubber composites. J. Appl. Polym. Sci. **135**, 47375 (2018)

Figures

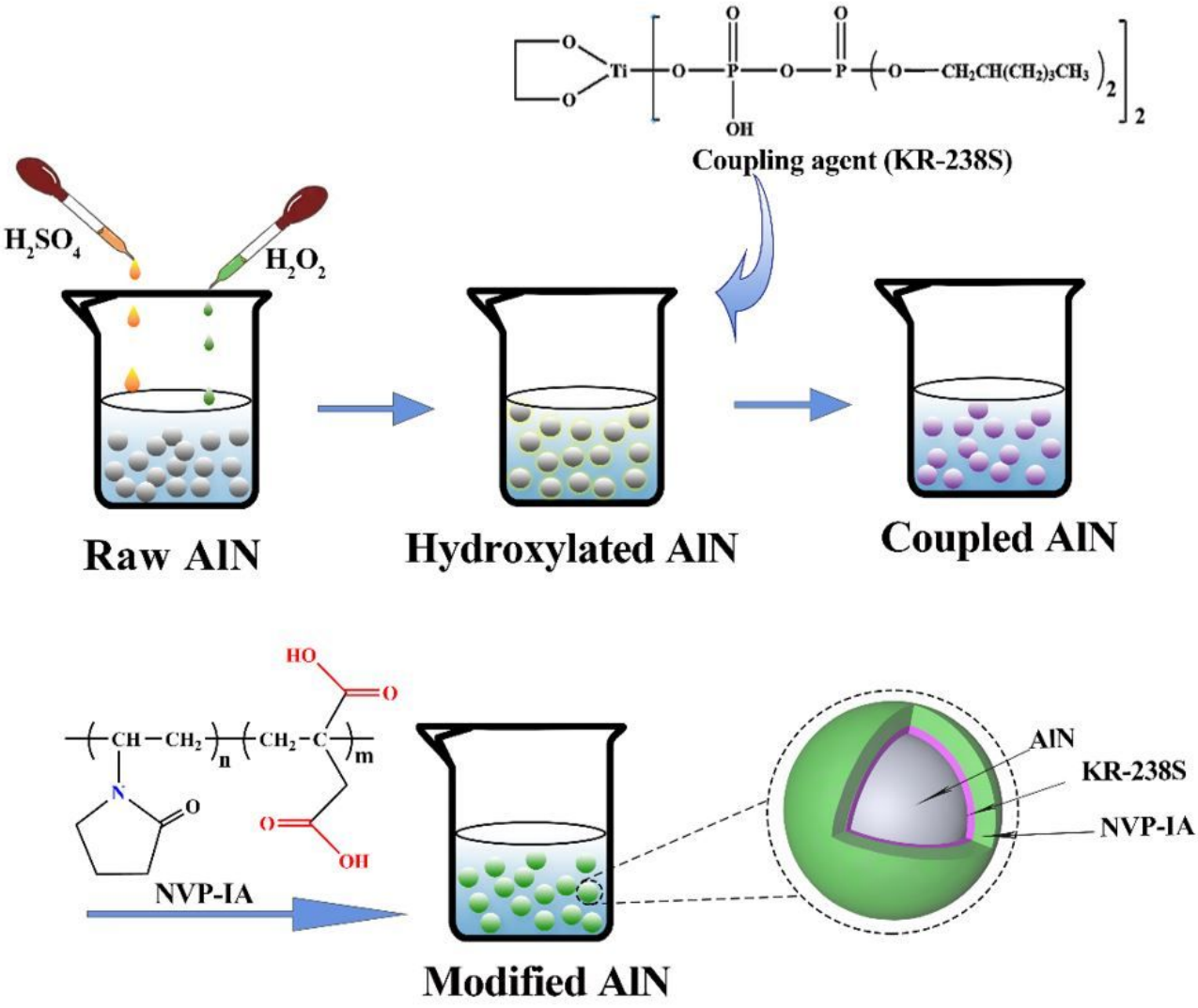

Figure 1

Preparation of hydrolysis-resistant AlN powders

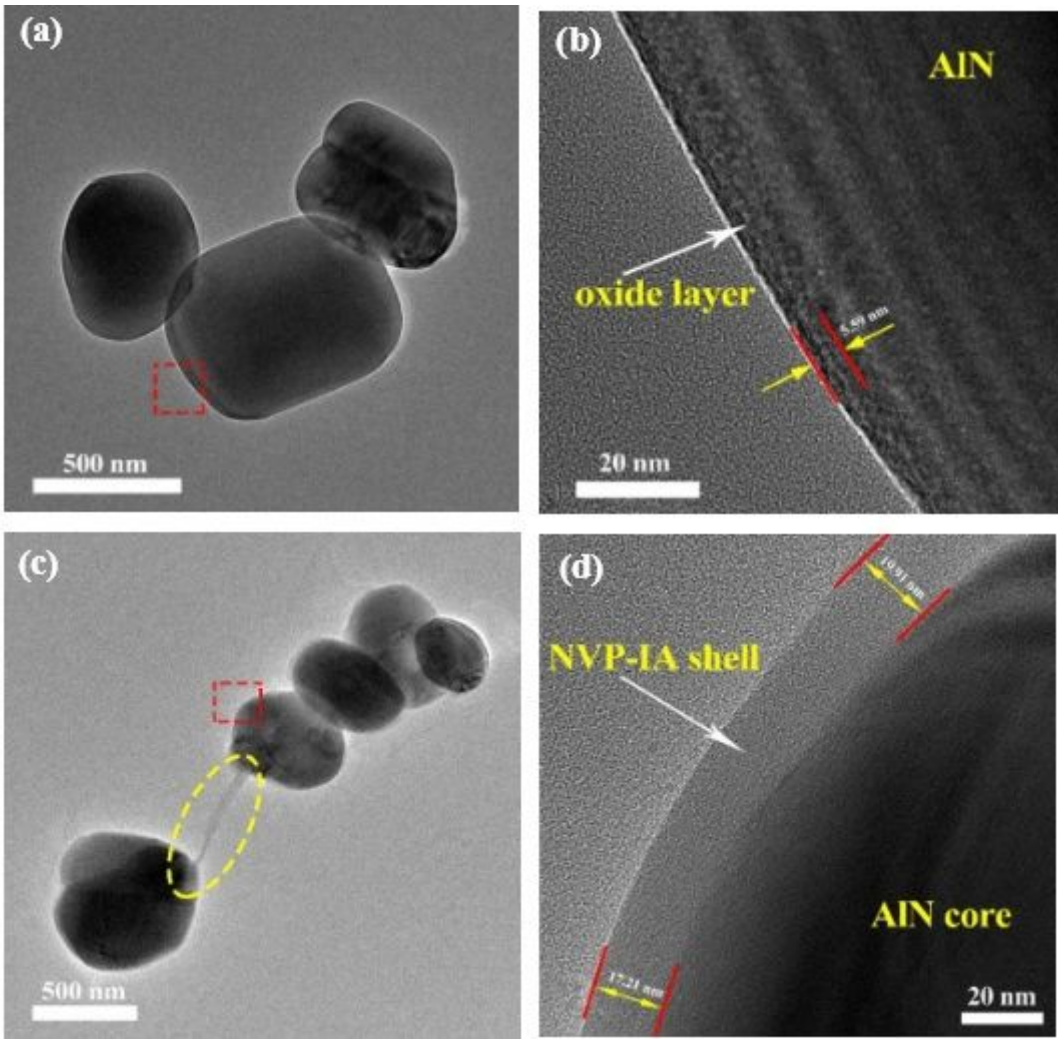

Figure 2

High-resolution TEM micrographs of (a) R-AlN powders (b) partial enlargement of R-AlN powders, (c) M-AlN powders, (d) partial enlargement of M-AlN powders

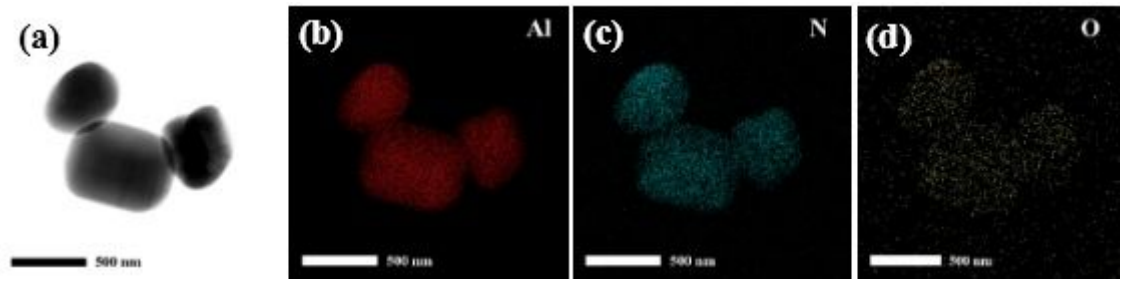

Figure 3

EDS Mapping spectrum of R-AlN (a) R-AlN, (b) Al distribution,

(c) N distribution, (d) O distribution

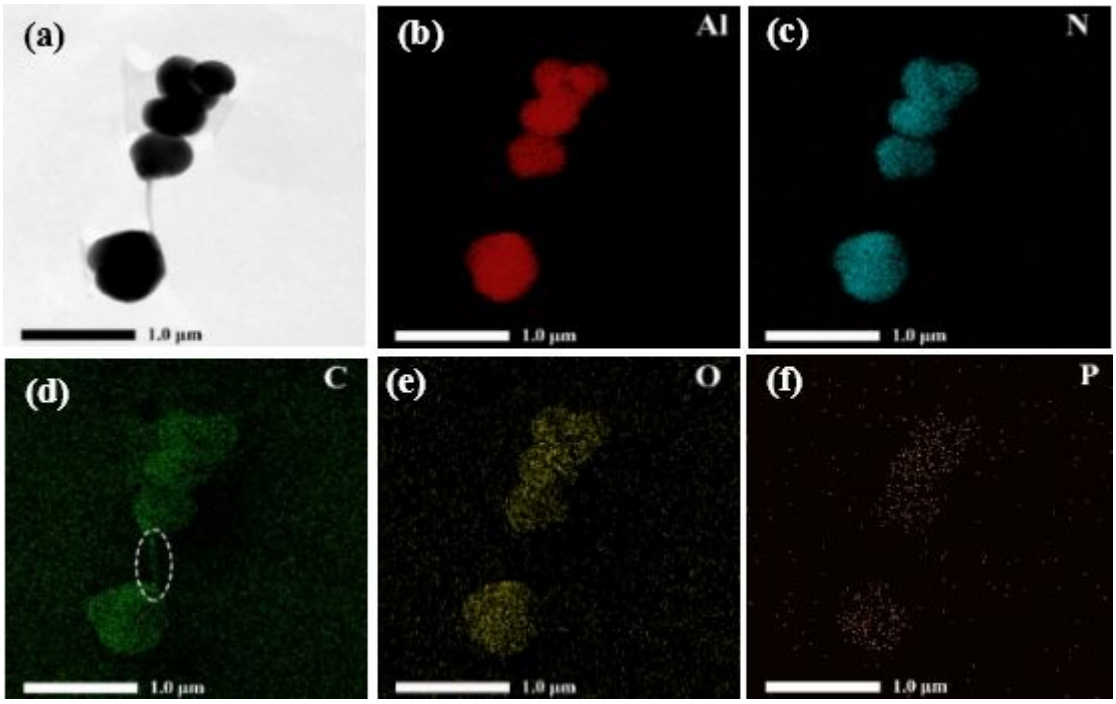

Figure 4

EDS mapping spectrum of M-AlN (a) M-AlN, (b) Al distribution, (c) N distribution, (d) C distribution, (e) O distribution, (f) P distribution

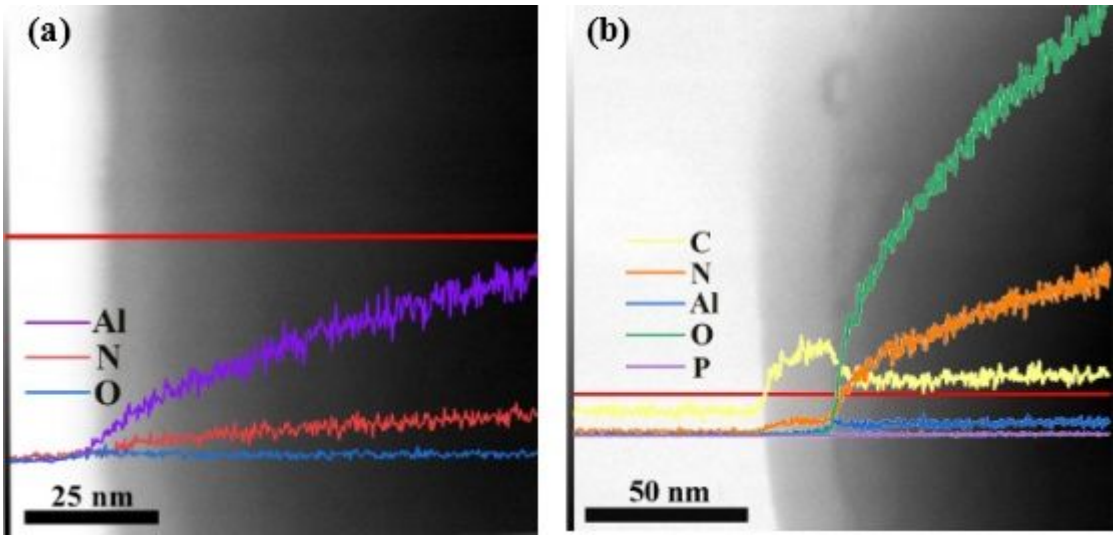

Figure 5

High-resolution TEM line-scanning micrographs of (a) R-AlN powders, (b) M-AlN polymers

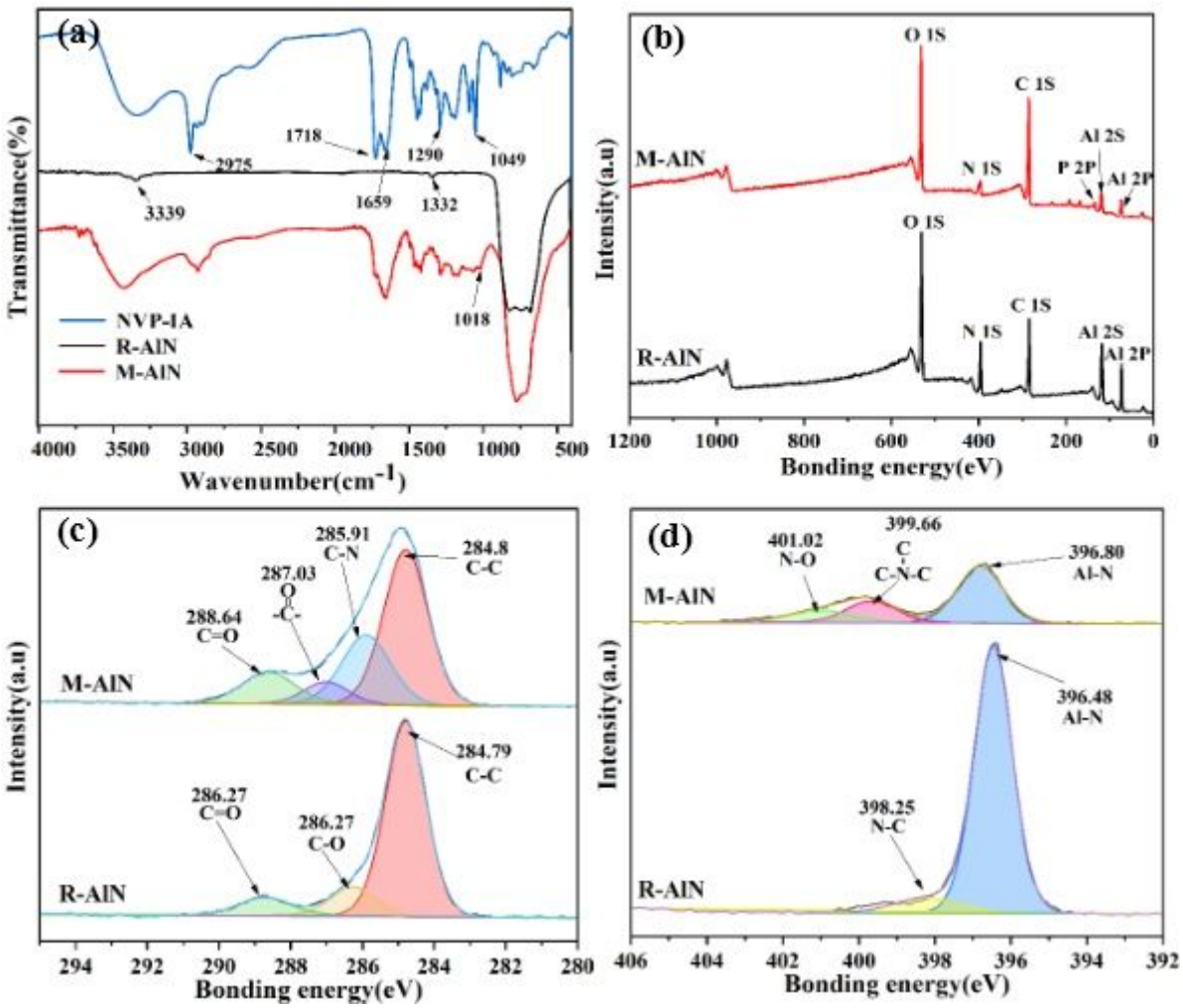

Figure 6

chemical bond structure of (a) FTIR spectra, (b) XPS qualitative full spectra,

(c) XPS C 1S spectra, (d) XPS N 1S spectra

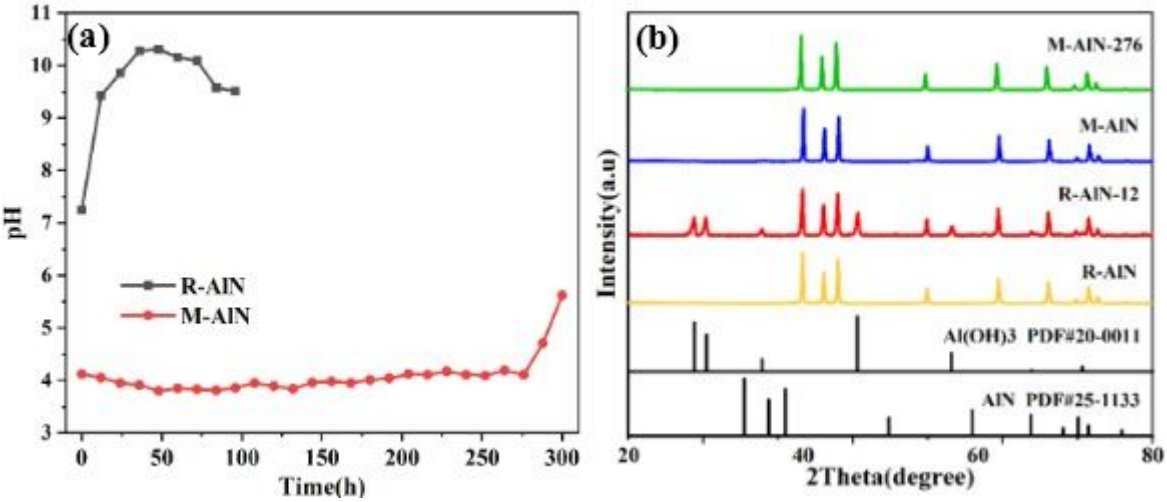

Figure 7

(a) pH change curve, (b) XRD comparison of AlN powders

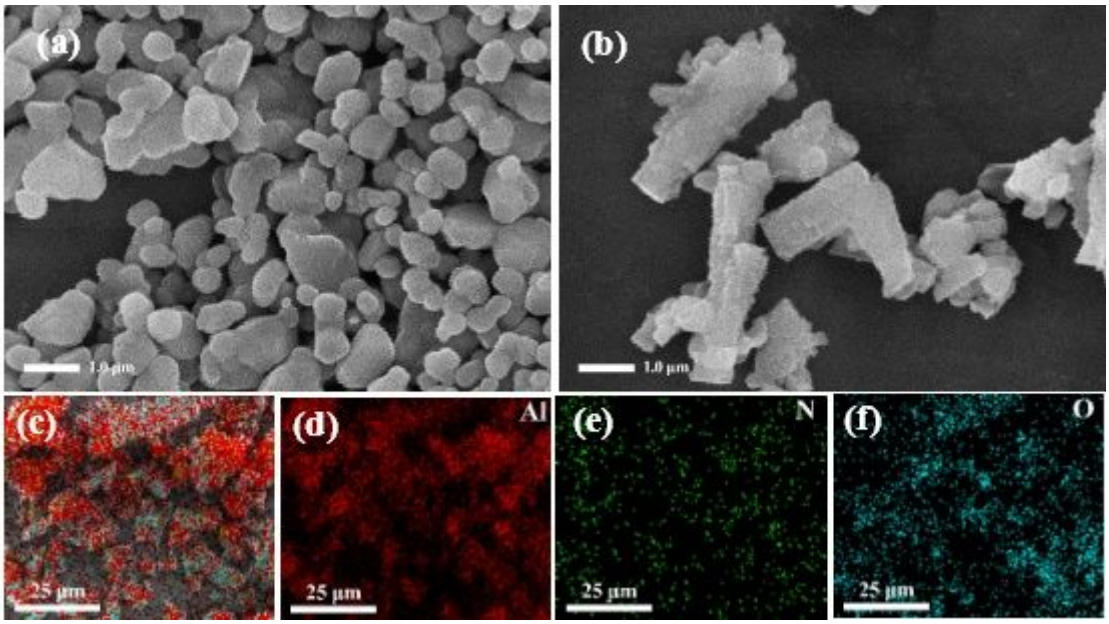

Figure 8

SEM images of (a) R-AlN, (b)R-AlN-12, EDS mapping spectrum of (c) R-AlN-12,

(d) Al of R-AlN-12, (e) N of R-AlN-12, (f) O of R -AlN-12

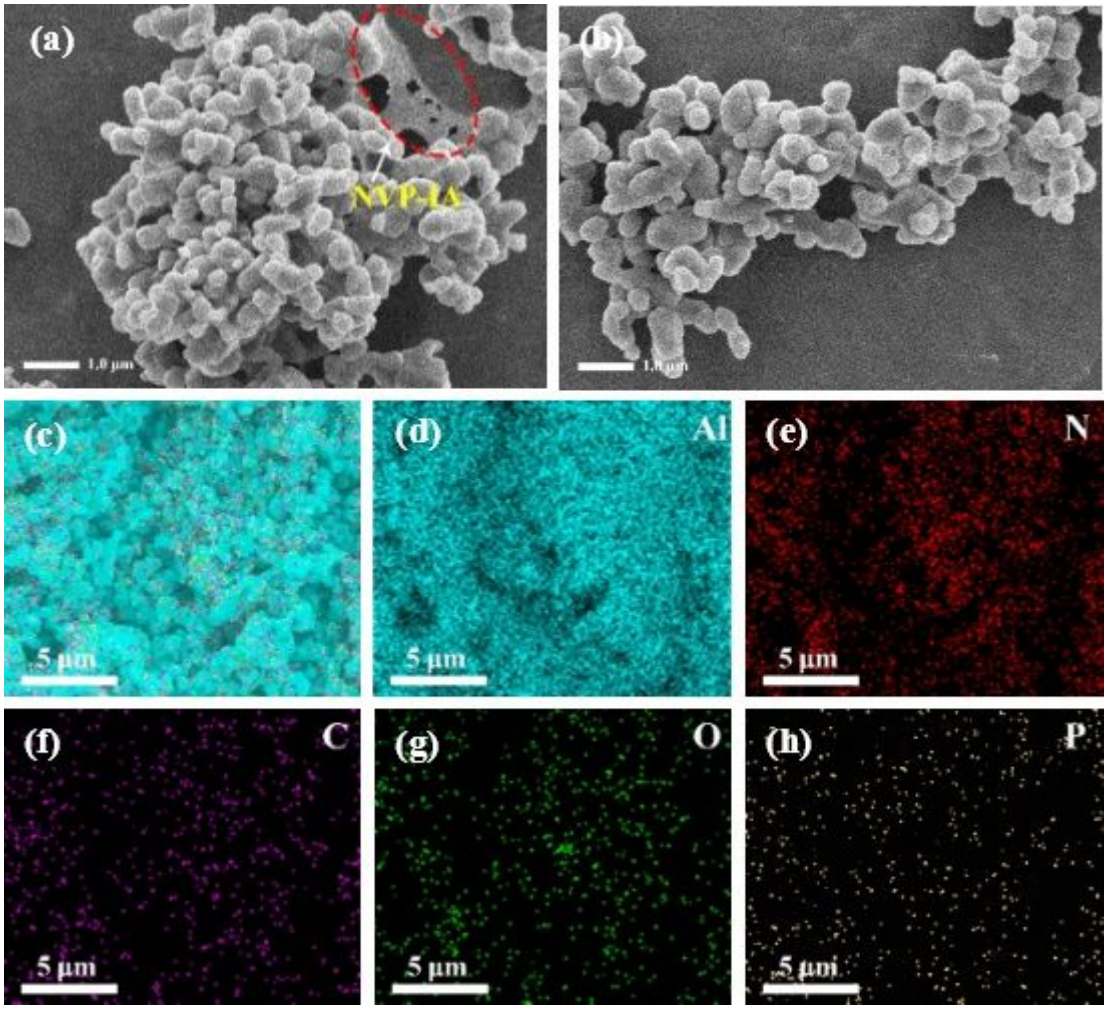

Figure 9

SEM images of (a) M-AlN, (b)M-AlN-276,

EDS mapping spectrum of (c)M-AlN-276, (d) Al of M-AlN-276, (e) N of M-AlN-276,

(f) C of M-AlN-276, (g) O of M-AlN-276, (h) P of M-AlN-276

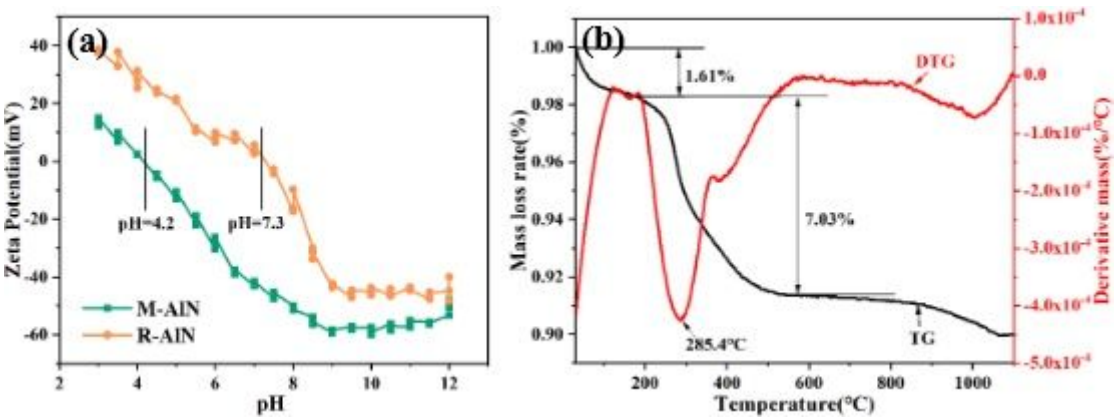

Figure 10

(a) Zeta potential vs pH value, (b) TG and DTG of M-AlN